XI Slip velocity and lift at finite Reynolds numbers

In this chapter we assemble results from direct numerical simulation, analysis and experiments that enter into an analysis of lift. We define and show that the slip angular velocity discrepancy is an important quantity that determines the equilibrium of a free particle in flows with a shear gradient. The equilibrium values of free particles lose stability as the shear Reynolds number is increased; they undergo turning point bifurcations leading to nonuniqueness and hysteresis.

▪ Equilibrium positions of neutrally buoyant and heavy particles

We have already noted that the experiments of Segré and Silberberg 1961, 1962 have had a big influence on fluid mechanics studies of migration and lift. They studied the migration of dilute suspensions of neutrally buoyant spheres in pipe flows at Reynolds numbers between 2 and 700. The particles migrate away from the wall and centerline and accumulate at 0.6 of a pipe radius.

The lift on heavier than liquid particles is also influenced by the factors that determine the equilibrium position of neutrally buoyant particles. The heavy particles must reach an equilibrium that balances the hydrodynamic lift and buoyant weight. If the buoyant weight is very small, the equilibrium position of the particles will be close to the value for the neutrally buoyant case. The effect of increasing the weight is to lower the equilibrium position whose zero is established for the case of zero buoyant weight.

Most attempts to explain the Segré-Silberberg effects have been based on linearized low Reynolds number hydrodynamics. Possibly the most famous of these attempts is due to Saffman 1965. There are a number of formulas like Saffman's that are in the form of U_s times a factor, which can be identified as a density times a circulation as in the famous formula $\rho U \Gamma$ for aerodynamic lift. A relatively recent review of such formulas can be found in McLaughlin 1991.

Formulas like Saffman's cannot explain Segré-Silberberg's observations, which require migration away from both the wall and the center. There is nothing in these formulas to account for the migration reversal near 0.6 of a radius. Moreover the slip velocity U_s, the angular slip velocity $\Omega_s = \Omega_p - \Omega_f = \Omega_p + \dot{\gamma}/2$, the particle velocity and the particle angular velocity, which are functionals of the solution are prescribed quantities in these formulas.

The fluid motion drives the lift on a free body in shear flow; no external forces or torques are applied. If there is no shear there is no lift. In Poiseuille flow there is not only a shear but a shear gradient. Gradients of shear (curvature) produce lateral forces. At the centerline of a Poiseuille flow the shear vanishes, but the shear gradient does not. To understand the Segré-Silberberg effect it is necessary to know that the curvature of the velocity profile at the center of Poiseuille flow makes the center of the channel an unstable position of equilibrium. A particle at the center of the channel or pipe will be driven by shear gradients toward the wall; a particle near the wall will lag the fluid and be driven away from the wall. An equilibrium radius away from the center and wall must exist. The effects of migration and lift which determine the equilibrium position of a particle in a Poiseuille flow were discussed as a perturbation of Stokes or Oseen flow by Ho and Leal 1974, Vasseur and Cox 1976, Schonberg and Hinch 1981 and Asmolov 1999.

This paper approaches the problem of migration and lift in a different way. Basically we have used direct numerical simulation (DNS) to formulate and validate a long particle model that gives a very good, completely explicit analytical approximation to the velocity and slip velocity of circular particles. DNS is used here as a diagnostic tool to analyze the role of the slip velocity, and the angular slip velocity on migration and lift. We are able in this way to establish a rather simple picture of lift and migration that in particular clarifies the role of the angular slip velocity, and is not restricted to low Reynolds numbers. Our analysis is carried out in two dimensions but should apply in principle to 3D, which is at present under study.

▪ Mechanism for lift

We can look at formulas for the lift on a particle in an inviscid fluid, which were discussed in chapter X, and which can be viewed as realizations of Rayleigh's lift formula (X.1) $L' = \rho U \Gamma$. A circular particle experiences a lift per unit length (X.4) $L' = 2\pi\rho a^2 U\Omega$; this may be compared with Auton's formula (X.8) for the L on a sphere rotating in a shear flow. $L = -^4/_3\ \rho a^3 \Omega_f U_s$ where $\Omega_f = -^1/_2\ du/dy$ is the angular velocity of the fluid.

If $du/dy > 0$ the sphere is lifted against gravity when the slip velocity U_s is positive; if U_s is negative the sphere will fall. Particles that lag the fluid migrate to streamlines with faster flow, particles which lead the fluid migrate to streamlines with slower flow.

There are rather striking differences between (X.8) and (X.4); first (X.4) depends on the angular velocity of the particle but (X.8) depends on the angular velocity of the fluid. Both formulas leave the slip velocity undetermined, U_s appears in (X.8) because of the shear, in (X.4), $U_f = 0$. The slip velocities have to be prescribed in these theories because the particle velocity is not determined by viscous drag; similarly the angular velocity of the particle cannot arise from torques arising from viscous shears. The effects of particle rotation cannot be obtained by the method of Auton 1987.

The lift formula $\rho U \Gamma$ captures the essence of the mechanism in which the motion of the particle relative to the fluid is such as to increase the pressure on the side of the particle as it moves forward.

The lift on a spherical or circular particle in a shear flow is different; there is no exterior agent to move and rotate the freely moving particle. Instead the particle is impelled forward and rotated by the shear flow. Previous theoretical studies and the simulations of Joseph and Ocando 2001 show that the relevant velocity is the slip velocity and the relevant circulation is proportional to an angular slip velocity discrepancy

$$\Gamma \propto \Omega_s - \Omega_{se} \tag{XI.1}$$

where Ω_{se} is the slip angular velocity in steady flow (equilibrium). This conclusion will be established in the sequel. For now we simply note that in the simulations the angular slip velocity discrepancy $\Omega_s - \Omega_{se} < 0$ when the cylinder is above the equilibrium (Segré-Silberberg) position and $\Omega_s - \Omega_{se} > 0$ when it is below the equilibrium (figure XI.8).

▪ Numerical simulation of migration and lift

In numerical experiments of solid-liquid flows we can examine physical effects one at a time; this cannot be done in real experiments. For the present application we look first at the effect on particle migration of controlling the angular velocity of the particle. In figure IX.8 we plotted the rise to equilibrium of a neutrally buoyant particle for three different values of the slip angular velocity

$$\Omega_s = \frac{\overset{\circ}{\gamma}}{2} + \Omega_p = \left\{ \frac{\overset{\circ}{\gamma}}{2},\ \Omega_{se},\ 0 \right\}. \qquad \text{(XI.2)}$$

The rise is the greatest when the particle angular velocity $\Omega_p = 0$ and the least when the particle angular velocity is equal to the local rate of rotation $\Omega_p = -\dot{\gamma}/2$. The rise of a heavier than liquid $\rho_p/\rho_f = 1.01$ circular particle is plotted in figure IX.8 for Reynolds number $R_w = \dot{\gamma}_w d^2/\nu = 5.4$ and for $R_w = 16.2$ in figure IX.9. The angular slip velocity $\Omega_{se} > 0$ is the equilibrium value that a free circular particle takes in torque-free motion when the angular acceleration vanishes. We call attention to the fact that $\Omega_{se} > 0$ is very small, and at equilibrium

$$\left| \frac{\overset{\circ}{\gamma}}{2} \right| > \left| \Omega_{pe} \right|, \qquad \Omega_{pe} \approx -\frac{\overset{\circ}{\gamma}}{2}. \qquad \text{(XI.3)}$$

In another constrained motion we fix the y position of the particle and compute the slip velocities and lift (figure X.6). A fixed particle with non-zero lift forces will migrate if the constraint is relaxed.

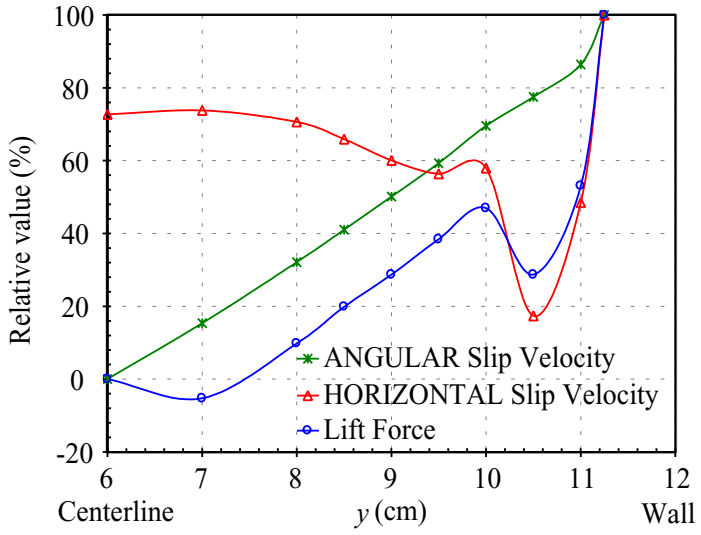

Figure XI.1. *FIXED PARTICLE: $R_w = 20$, $\rho_s/\rho_f = 1$. Steady state relative values for the lift force and the slip velocities. In the region close to the wall, the lift force and the horizontal slip velocity have a similar non-linear behavior. In the region close to the centerline, the lift force appears to be*

proportional to the angular slip velocity. Therefore, the lift force may be expressed as a function of the slip velocity product $L = L(\mathbf{U}_s, \boldsymbol{\Omega}_s)$.

▪ Long particle model

Joseph 2001 proposed a model problem for the velocity of a long particle in Poiseuille flow (also see Choi and Joseph, 2001). We replaced the circular particle of diameter *d* with a long rectangle whose short side is *d*. The rectangle is so long that we may neglect the effects of the ends of the rectangle at sections near the rectangle

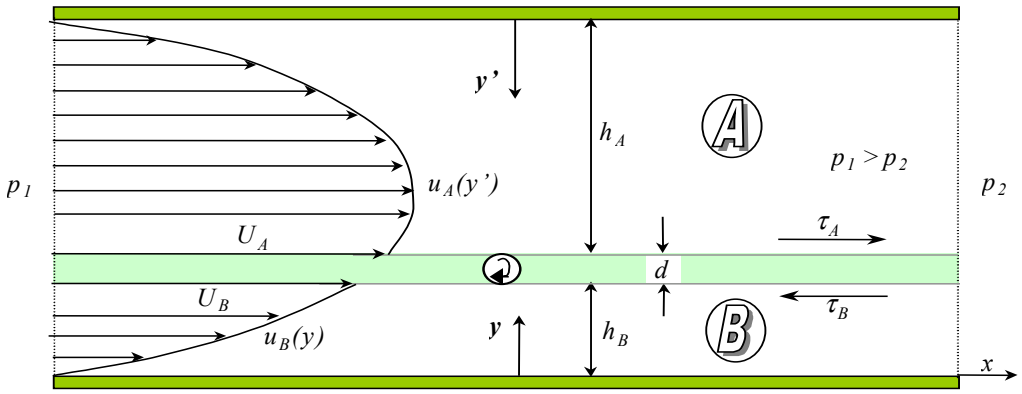

Figure XI.2*. Sketch of flow field under consideration and variables involved in the long particle model.* $W = h_A + h_B + d$ *is the channel height.*

center. In that model the long particle was assumed to be rigid but it was noted that a more realistic model could be obtained by letting the long particle shear. We could choose this shear to be the same as the shear rate of the circular particle in the approximation in which $\Omega_p = -\frac{1}{2}\dot{\gamma}$ (figure XI.2).

The long particle model is meant to represent the constrained forward motion with y_p fixed after transients have decayed and steady flow is achieved. The model may be compared with the numerical simulation satisfying the fluid equations (IX.6) with $\partial \boldsymbol{u}/\partial t = 0$, the *x*-component of (IX.7) with $\mathrm{d}\boldsymbol{u}/\mathrm{d}t = 0$

$$\bar{p}\boldsymbol{e}_x + \boldsymbol{e}_x \frac{1}{V_p} \oint \{-p\boldsymbol{1} + 2\eta \boldsymbol{D}[y]\} \cdot \boldsymbol{n} d\Gamma = 0 \qquad \text{(XI.4)}$$

and (IX.8) with $\mathrm{d}\boldsymbol{\Omega}/\mathrm{d}t = 0$. The *y*-component of (IX.7) gives the balance of buoyant weight and lift; the particle density enters into this balance through the buoyancy term. It follows that buoyancy and the particle density do not enter into the constrained simulations, which determine the steady motion of the fluid and the forward motion of the particle, and they do not enter into the long particle model, which approximates the simulation.

The model leads to an explicit expression for the particle velocity and slip velocity in which vertical migration is suppressed. Since the simulation and the model do not depend on ρ_p, there

is a sense in which the results given here are universal. However, each constrained simulation is realizable for a density given by $\rho_p = \rho_f + L_e/V_p^g$ in which the *y*-component of (IX.7) is satisfied.

The forces acting on the long particle are the force due to pressure acting on the sides perpendicular to the flow, and the force due to shear stress acting on the sides parallel to the flow (figure XI.2). The former force is always positive, while the latter may be positive or negative depending if the fluid is faster than the particle or vice versa,

$$(\tau_A + \tau_B)l + (p_1 - p_2)d = 0 \tag{XI.5}$$

$$\tau_A + \tau_B + \bar{p}d = 0\,, \quad \bar{p} = \frac{(p_1 - p_2)}{l} \tag{XI.6}$$

where the shear stresses are defined by

$$\tau_A = -\eta \frac{du_A}{dy'}(h_A)\,, \quad \tau_B = -\eta \frac{du_B}{dy}(h_B) \tag{XI.7}$$

The velocity profiles above and below the long particle are given by

$$u_A(y') = \frac{\bar{p}}{2\eta} y'(h_A - y') + \frac{U_A y'}{h_A} \tag{XI.8}$$

$$u_B(y) = \frac{\bar{p}}{2\eta} y(h_B - y) + \frac{U_B y}{h_B} \tag{XI.9}$$

where different velocities (U_A, U_B) were assumed for the top and bottom walls to take into account the angular speed of the circular particle. The relation between them is given by

$$U_A - U_B = \tfrac{1}{2}\dot{\gamma}\left(h_B + \tfrac{1}{2}d\right)d\,, \tag{XI.10}$$

where $\dot{\gamma}(y)$ is the shear rate for the undisturbed flow (without the particle), given by

$$\dot{\gamma}(y) = \frac{\mathrm{d}u}{dy} = \frac{\bar{p}}{2\eta}(W - 2y)\,. \tag{XI.11}$$

The shear rate on the particle's sides parallel to the flow may be evaluated from (XI.8), (XI.9) and (XI.10),

$$\frac{\mathrm{d}u_A}{\mathrm{d}y'}(h_A) = -\frac{\bar{p}}{2\eta}h_A + \frac{U_B}{h_A} + \frac{\dot{\gamma}\left(h_B + \frac{1}{2}d\right)}{2}\frac{d}{h_A} \tag{XI.12}$$

$$\frac{\mathrm{d}u_B}{\mathrm{d}y}(h_B) = -\frac{\bar{p}}{2\eta}h_B + \frac{U_B}{h_B}\,. \tag{XI.13}$$

Substituting, recursively, (XI.12) and (XI.13) in (XI.7), and then the resultant equation in (XI.6), we find that at the top and bottom of the long particle (diameter *d*):

$$U_A = \frac{(\bar{p}/\eta)(2d + h_A + h_B)h_A h_B + \dot{\gamma}(h_B + d/2)\,h_A d}{2(h_A + h_B)} \tag{XI.14}$$

$$U_B = \frac{(\bar{p}/\eta)(2d + h_A + h_B)h_A h_B - \dot{\gamma}(h_B + d/2)\,h_B d}{2(h_A + h_B)} \tag{XI.15}$$

The average particle velocity is:

$$U_p = \tfrac{1}{2}(U_A + U_B) = \frac{(\bar{p}/\eta)(2d + h_A + h_B)h_A h_B - \dot{\gamma}(h_B + d/2)\,(h_B - h_A)\,\tfrac{1}{2}d}{2(h_A + h_B)}. \tag{XI.16}$$

The undisturbed flow field (without the particle) can be written as:

$$u(y) = \frac{\bar{p}}{2\eta} y(W - y) \tag{XI.17}$$

At the position where the center of the particle is located ($y_p = h_B + \tfrac{1}{2}d$), the undisturbed fluid velocity is:

$$u(h_B + \tfrac{1}{2}d) = \frac{\bar{p}}{2\eta}(h_B + \tfrac{1}{2}d)\,(h_A + \tfrac{1}{2}d) \tag{XI.18}$$

The particle slip velocity can be defined as:

$$U_s = u(h_B + \tfrac{1}{2}d) - U_p \tag{XI.19}$$

which can be written as:

$$U_s = \frac{(\bar{p}/\eta)\left[(h_A + h_B)(h_B + \tfrac{1}{2}d)(h_A + \tfrac{1}{2}d) - (2d + h_A + h_B)h_A h_B\right] + \dot{\gamma}(h_B + \tfrac{1}{2}d)(h_B - h_A)\,\tfrac{1}{2}d}{2(h_A + h_B)} \tag{XI.20}$$

The channel height W and the position h_A and h_B satisfy the following conditions:

$$\begin{cases} h_A = W - (h_B + d), \\ h_A + h_B = W - d, \end{cases} \qquad y_p = h_B + \tfrac{1}{2}d$$

and the shear rate at the particle center is

$$\dot{\gamma}(h_B + \tfrac{1}{2}d) = \frac{\bar{p}}{2\eta}(W - d - 2h_B)\ . \tag{XI.21}$$

Then the slip velocity can be simplified:

$$\begin{aligned} U_s &= \frac{\bar{p}}{2\eta(h_A + h_B)}\left[(h_A + h_B)(h_B + \tfrac{1}{2}d)(h_A + \tfrac{1}{2}d) - (2d + h_A + h_B)h_A h_B + \tfrac{1}{2}(h - d - 2h_B)(h_B - h_A)\tfrac{2}{2}d\right] \\ &= \frac{\bar{p}}{2\eta(W - d)}\left[d\left(\tfrac{1}{2}W - y_p\right)^2 + \tfrac{1}{4}d^2(W - d)\right] \geq 0 \end{aligned} \tag{XI.22}$$

when $d \to 0$, we can get $U_s \to 0$.

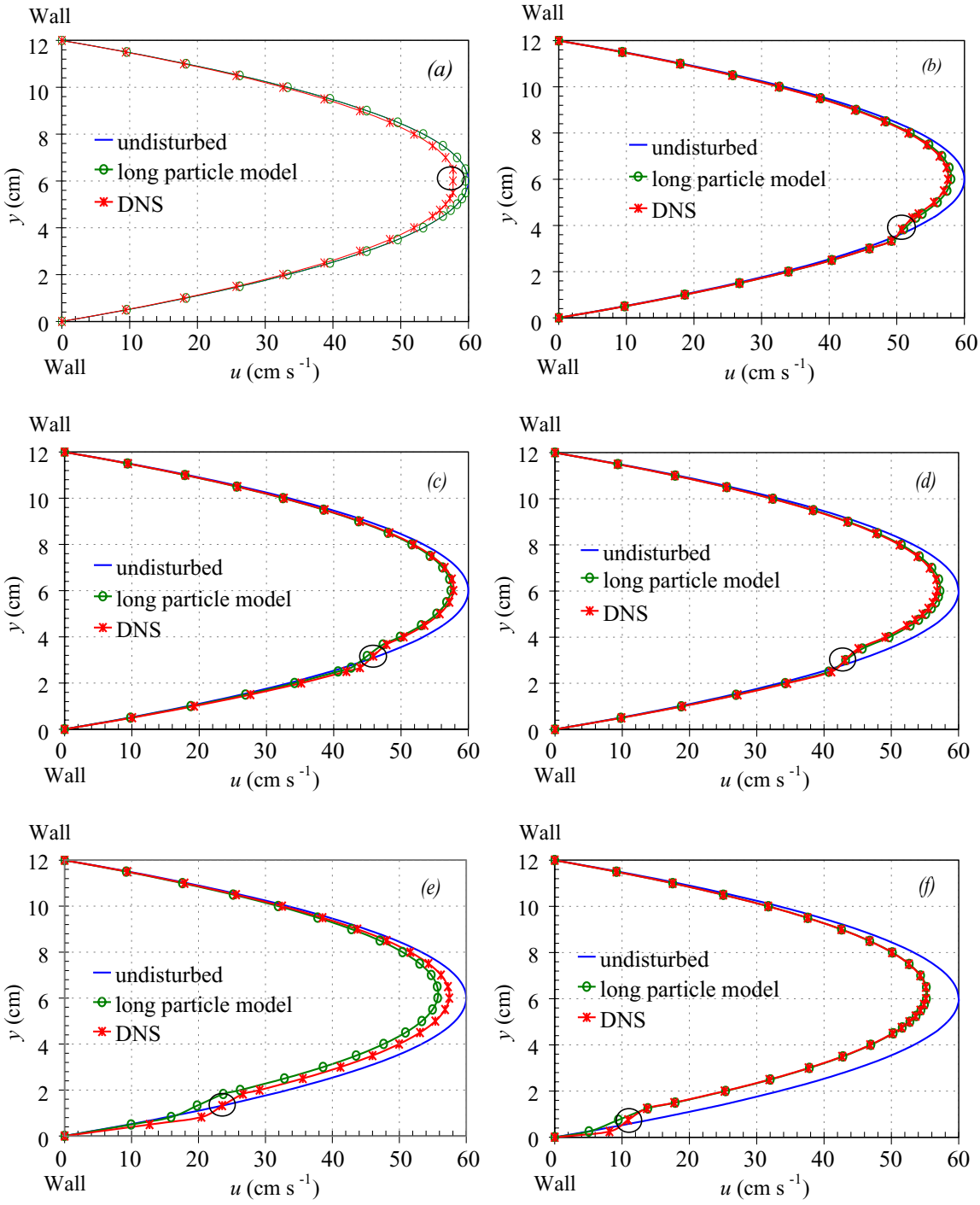

Figure XI.3. *Velocity profiles through the center* y_p *of a particle and the particle velocity at* $R = 20$. *The velocity profiles of the undisturbed flow, of the DNS simulation and the long particle model are compared:* (a) *centerline* $y_p = 6.0\,cm$, (b) *the unique equilibrium position when* $\rho_p/\rho_f = 1.005$ $(y_p = 3.834\,cm)$, (c) *the higher equilibrium position when* $\rho_p/\rho_f = 1.01$ $(y_p = 3.165\,cm)$, (d) $y_p = 3.0\,cm$, (e) *the lower equilibrium position when* $\rho_p/\rho_f = 1.01$ $(y_p = 1.323\,cm)$, (f) $y_p = 0.75\,cm$. *The centerline of* (a) *is unstable.*

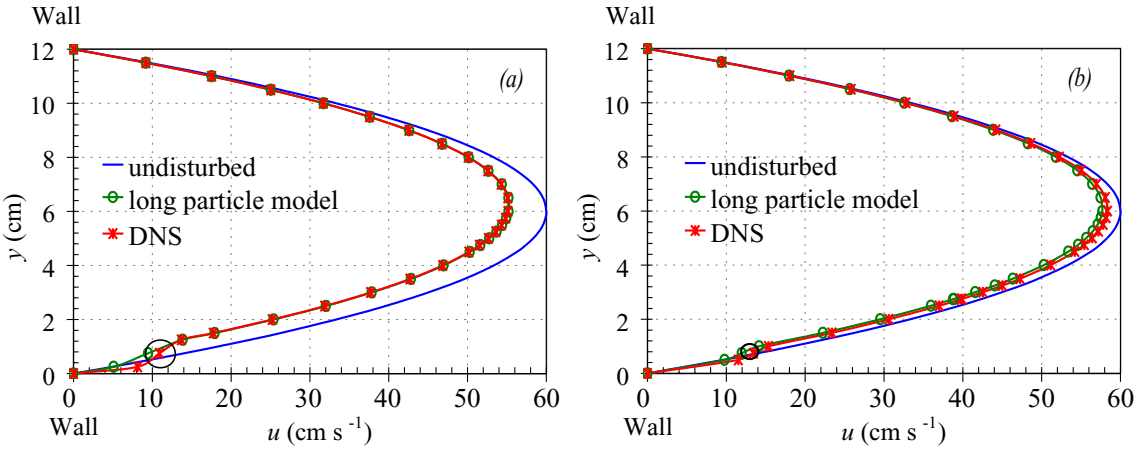

Figure XI.4. *Velocity profiles at steady state on a line through the center of a particle at* $y_p = 0.75\,cm$, $R = 20$. (a) *reference size* ($d = 1.0\,cm$), (b) *small particle* ($d = 0.5\,cm$). *As the particle is smaller, the difference between disturbed and undisturbed velocity profiles is smaller.*

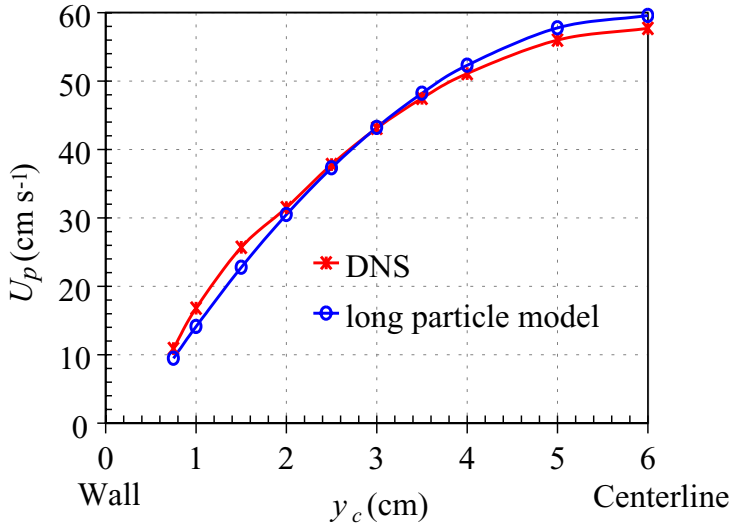

Figure XI.5. *Particle velocity* vs. *particle position.*

A comparison of the long particle model with DNS for a circular particle is given in figure XI.3 and XI.4. In these constrained simulations we fix the y position of the particle and compute the dynamic evolution to equilibrium at $R = 20$. The diameter of the particle in figure XI.3 is 1 cm and in figure XI.4 it is 0.5 cm. The profiles in the figures are at equilibrium and on a cross-section through the center of the particle. The agreement is rather better than might have been anticipated given the severe assumptions required in the model. The agreement is quite good away from the centerline, even close to the wall. Equations (XI.6-XI.10) can be recommended for an analytical approximation for the velocity of a circular particle in Poiseuille flow.

In figure XI.5, we compare the particle velocity from the simulation with the long particle model. In figure XI.6, we compare the slip velocity, and in Figure XI.7 we show how nearly the particle angular velocity is given by $-\frac{1}{2}\dot{\gamma}(y_p)$.

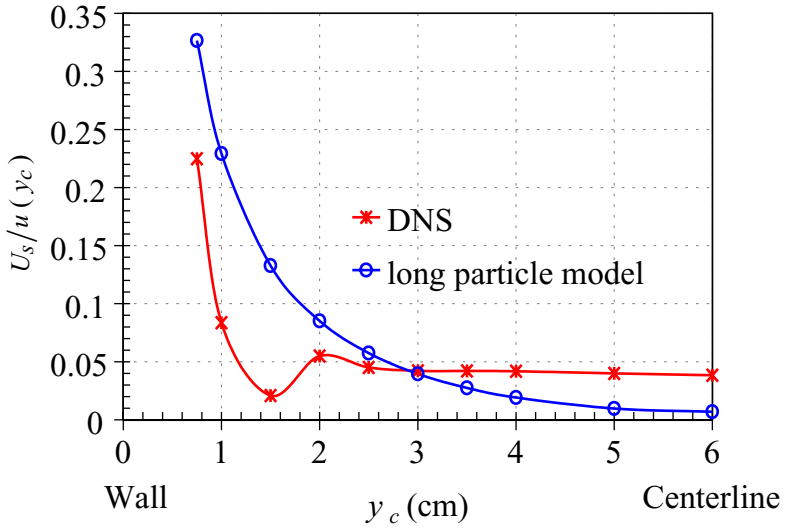

Figure XI.6. *Slip velocity/fluid velocity ratio* vs. *particle position at* $R = 20$. *Slip velocity evaluated using DNS results* vs. *slip velocity in the long particle model. These are relative values of the slip velocity,* U_s, *with respect to the fluid velocity on the undisturbed flow at the particle center* $u(y_p)$. *The largest discrepancy is at about* $\frac{1}{4}$ *the distance from the wall to the centerline.*

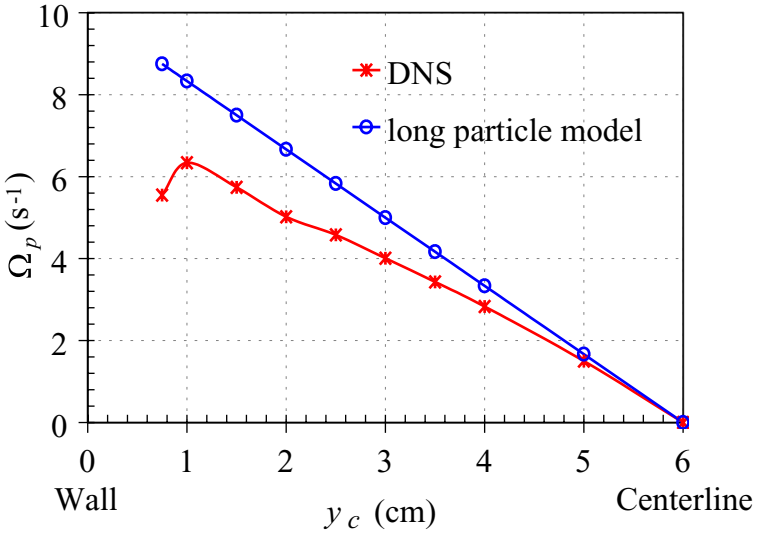

Figure XI.7. *Particle angular velocity,* Ω_p *at* $R = 20$. *The angular velocity of the particle is approximated in the long particle model as half the value of the shear rate on the undisturbed flow evaluated at particle's center position* $\Omega_p\big|_{LPM} = -\frac{1}{2}\dot{\gamma}(y_p)$.

▪ Slip velocities, angular slip velocities and lift for neutrally buoyant circular particles

Multiple equilibrium solutions do not appear at moderate numbers when $\rho_p = \rho_f$, $R_G = 0$; the equilibrium solutions are unique. Figures XI.8, XI.9 and XI.10 show the evolution to equilibrium, at $R = 10$, of a neutrally buoyant particle started at the wall and at the centerline from an initial condition of rest. No matter where the particle is released it will migrate to a unique equilibrium solution at $y_e = 4.18\,\text{cm}$.

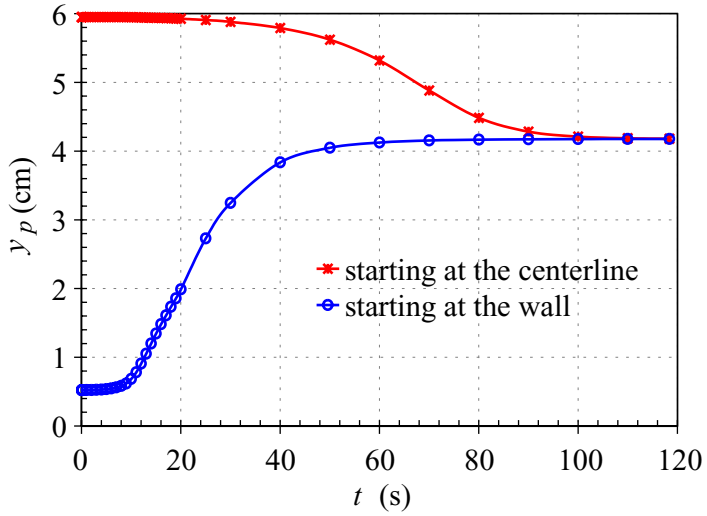

Figure XI.8. *Migration of a neutrally buoyant particle in an unconstrained simulation at* $R = 10$.

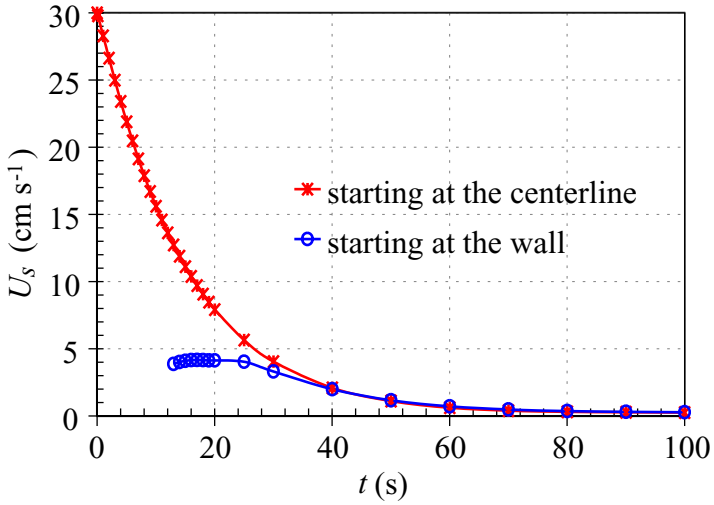

Figure XI.9. *Evolution of the slip velocity of the particle whose trajectory is shown in figure XI.8. The slip velocity evolves to zero through positive values whether the particle is started above or below the equilibrium position. The slip velocity discrepancy* $U_s - U_{se} > 0$, $U_{se} = 0.148\,\text{cm s}^{-1}$.

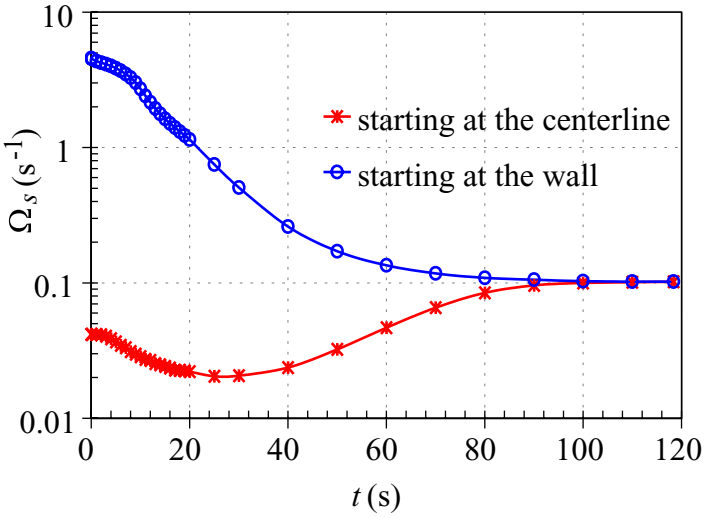

Figure XI.10. *Evolution of the angular slip velocity of a neutrally buoyant particle at* $R = 10$ *to equilibrium (see figure XI.8). The angular slip velocity function evolves without crossing the equilibrium value. When the angular slip velocity is below the equilibrium value, the particle moves downward. When the angular slip velocity is above the equilibrium value, the particle moves upward.*

In figure XI.9, we show the evolution of the slip velocity to equilibrium. The slip velocity is positive and of course the greatest for a particle released from rest at the centerline.

In figure XI.10, we show that the angular slip velocity is smaller than its equilibrium value when the particle is above the equilibrium position and, is larger than its equilibrium value when it is below the equilibrium position. The angular slip velocity discrepancy

$$\Omega_s - \Omega_{se}$$

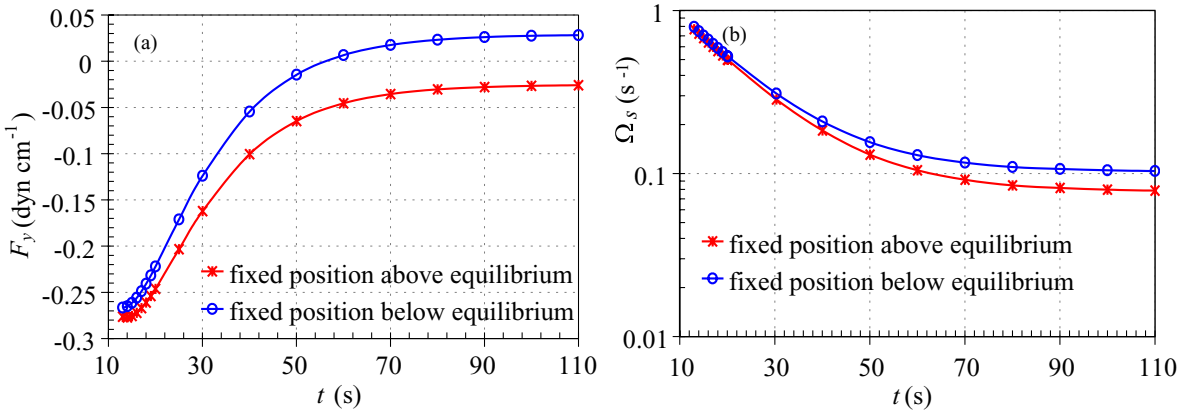

Figure XI.11. (a) *Lift and* (b) *angular slip velocity in constrained simulations of a particle fixed above and below equilibrium. The sign of the lift correlates perfectly with the sign of the angular slip velocity discrepancy.* $R = 10$, $y_p = 4.16$ *and 4.19 cm,* $y_e = 4.18$ cm.

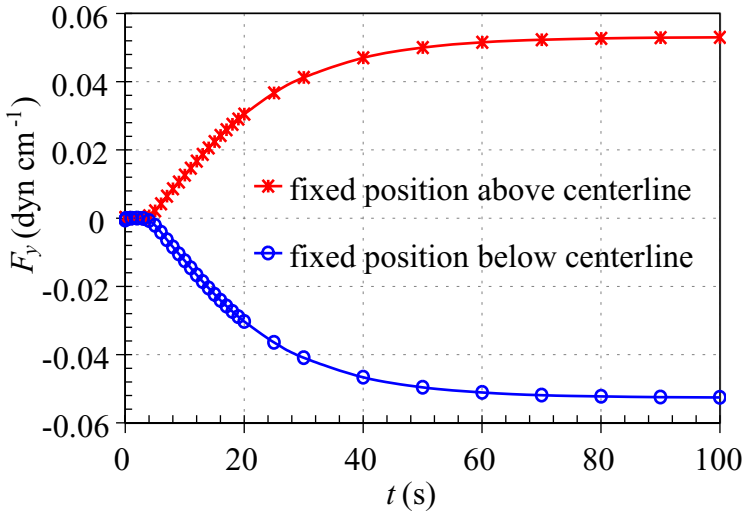

Figure XI.12. *Evolution of the lift on a particle at a fixed position at* $R = 10$ *slightly above,* $y_p = 6.05$ cm *and below,* $y_p = 5.95$ cm, *the centerline. The lift pushes the particle away from the centerline.*

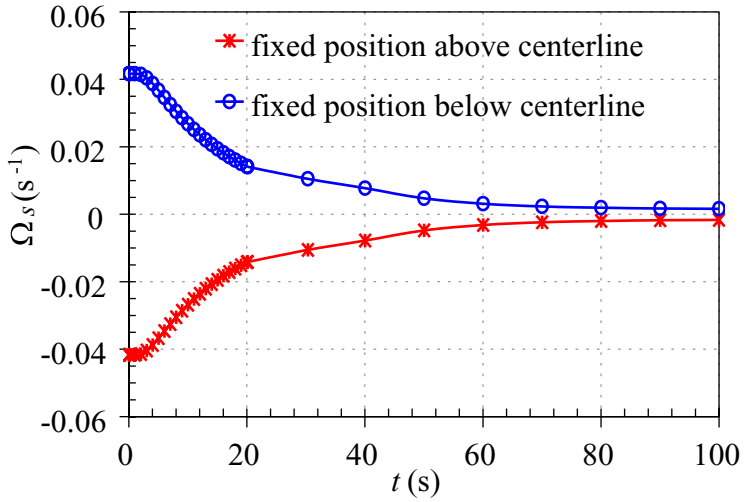

Figure XI.13. *Evolution of the angular slip velocity in a constrained simulation for particles at* $y_p = 5.95$ cm *and 6.05 cm when* $R = 10$. *The evolution is to a steady state with the following properties: when the angular slip velocity is below the equilibrium value, the particle moves upward. When the angular slip velocity is above the equilibrium value, the particle moves downward. This behavior is the opposite of the previous cases, because the previous cases were stable equilibrium positions, and therefore, the force field around them is the opposite.*

where Ω_{se} is the angular slip velocity at equilibrium, changes sign with the lift across the equilibrium.

In figure XI.11, we carry out a constrained simulation in which the circular particle is fixed at a position slightly above and slightly below the value of equilibrium. This figure shows that the sign of the angular slip velocity discrepancy changes with the sign of the lift, which is positive for particles below and negative for particles above the equilibrium.

In figures XI.12 and XI.13 are shown the evolution of the lift and angular slip velocity, respectively, from constrained simulations at fixed positions slightly above and slightly below the channel centerline. Figure XI.13, shows that the angular slip velocity discrepancy is negative when the particle is above the centerline and is positive when it is below the centerline. The discrepancy changes sign in both the stable and unstable cases, but the sign of the discrepancy is opposite in the two cases.

In figure XI.14, we have plotted the resultant constrained dynamical simulation comparing distributions of the normalized slip velocity, the angular slip velocity and lift for a neutrally buoyant particle are computed at each fixed position y_p for $R = 20$.

ρ_p / ρ_f	y_e (cm)	
	Starting at centerline	Starting close to wall
1.000	4.560	4.560
1.005	3.834	3.834
1.010	3.165	1.323

Table XI.1. *Position of equilibrium when* $R = 20$.

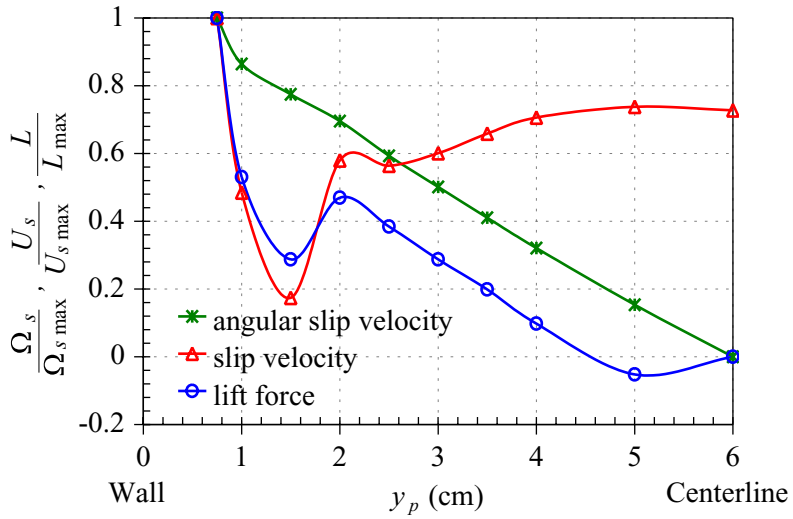

Figure XI.14. *Slip velocities and lift for neutrally buoyant particle at* $R = 20$. *Steady-state relative values for the lift force and the slip velocities. Dotted lines correspond to unstable equilibria. In the region close to the wall, the lift force and the slip velocity have a similar nonlinear behavior. In the region close to the centerline, the lift force appears to be proportional to the angular slip velocity.*

▪ Slip velocities, angular slip velocities and lift for non-neutrally buoyant circular particles

The qualitative results, which were established in the previous section hold for heavier and lighter than fluid particles. The slip velocity and angular slip velocity are positive and the angular

slip velocity discrepancy changes sign across y_e, where y_e is the place where the lift discrepancy

$$\mathcal{L} = L - \tfrac{1}{4}\left(\rho_p - \rho_f\right)\pi d^2 g \qquad \text{(XI.23)}$$

in two dimensions vanishes. For heavier than liquid particles, the position of equilibrium moves closer to the bottom wall, and for values of ρ_p/ρ_f larger than a critical two equilibrium heights exist (table XI.1).

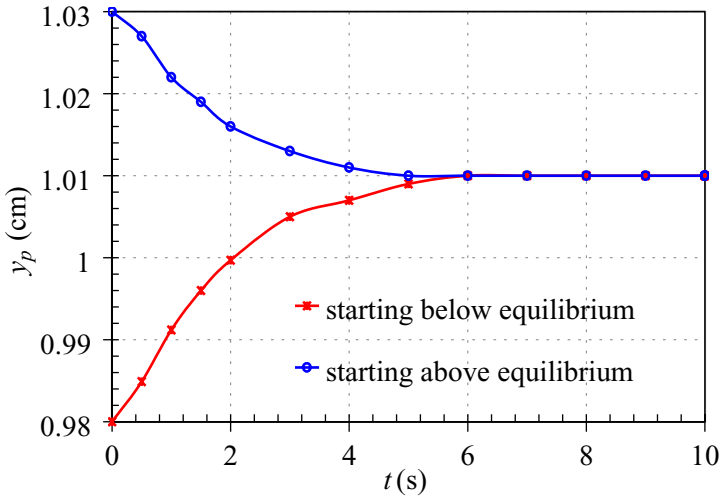

***Figure XI.15**. Particle height about equilibrium for a heavier-than-fluid particle ($\rho_p/\rho_f = 1.01$, $R = 10$). The initial condition was the steady state solution from a constrained simulation at the initial height.*

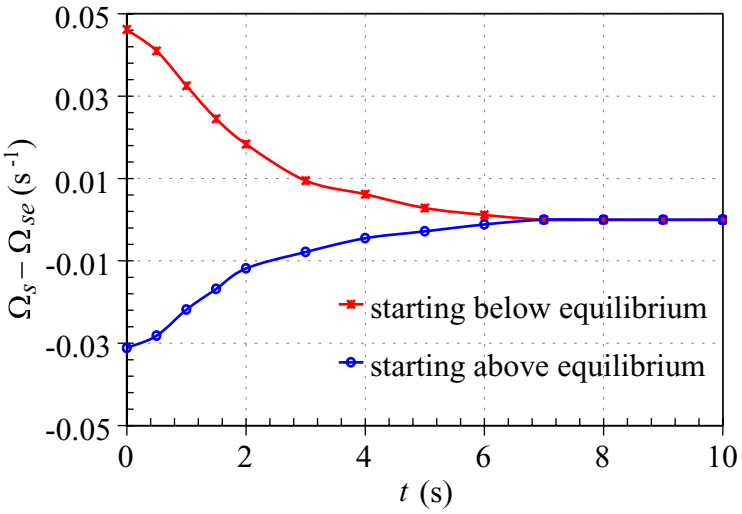

***Figure XI.16**. Angular slip velocity discrepancy about equilibrium for a heavier than fluid particle ($\rho_p/\rho_f = 1.01$, $R = 10$). The evolution on the angular slip velocity discrepancy is consistent with the evolution on the particle height.*

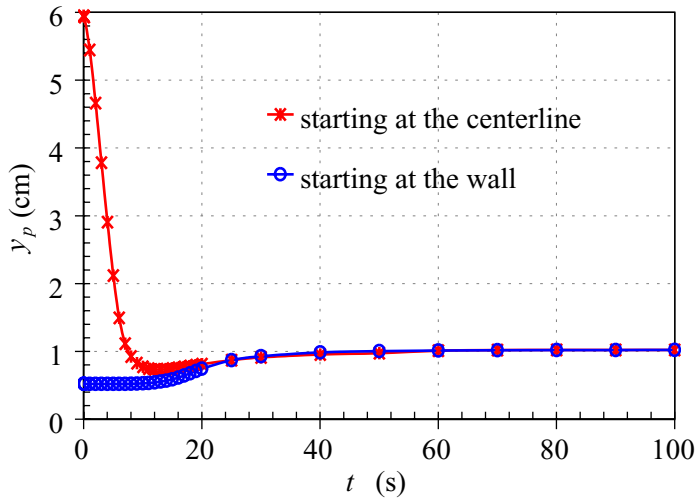

***Figure XI.17**. Migration from steady flow of a heavy particle $\rho_p/\rho_f = 1.01$ starting at rest near the wall and centerline at $R = 10$ ($R_G = 9.8$). The particle starting at the centerline crosses the equilibrium position and then moves upward.*

Figures XI.15 and XI.16 are plots of the migration to equilibrium of particles starting above and below but near to equilibrium when $R = 10$ and $R_G = 9.8$ corresponding $\rho_p/\rho_f = 1.01$. Figure XI.15 shows that the particle migrates to the same equilibrium whether it starts from above or below the position of equilibrium. Figure XI.16 is a plot of the angular slip velocity discrepancy versus time; it shows that the angular slip velocity discrepancy changes sign across the position of the equilibrium.

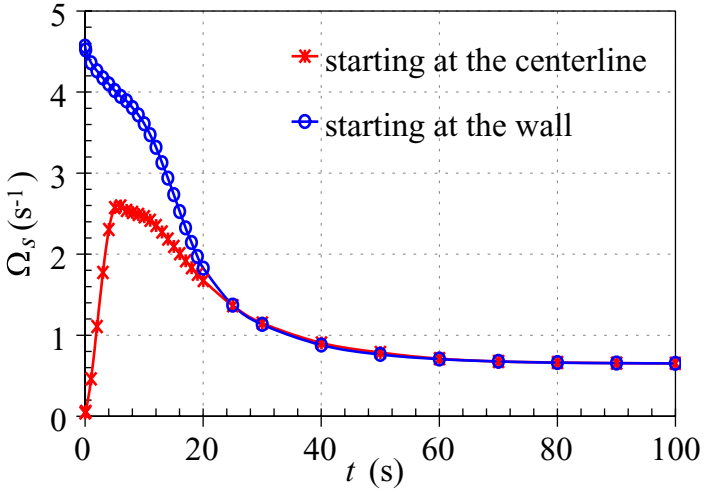

***Figure XI.18**. Evolution of the particle angular slip velocity of a heavier than fluid particle $\rho_p/\rho_f = 1.01$ starting at rest near the wall and centerline at $R = 10$, $R_G = 9.8$. For the particle starting at the centerline, the angular slip velocity function crosses the equilibrium value. When the angular slip velocity is below the equilibrium value, the particle moves downward. When the angular slip velocity is above the equilibrium value, the particle moves upward. A change in the sign of the angular slip velocity discrepancy is evident at early times when the particle falling from the centerline crosses the equilibrium; after this both particles are below the equilibrium and have essentially the same angular slip velocity.*

Figures XI.17 and XI.18 treat the same problem as in figures XI.15 and XI.16 but with a different initial condition. In figure XI.17, the particle is started from rest near the wall and the centerline

Figure XI.19 treats the problem of slip velocity and lift for the case $R = 20$ and $R_G = 9.8$ ($\rho_p / \rho_f = 1.01$) in which there are two stable equilibrium heights. In the dynamical simulation of a particle started from steady flow near the centerline, the particle migrates downward to the higher position of equilibrium and the angular velocity discrepancy is negative. When the particle is started from the wall it migrates upward to the lower position of equilibrium and the slip angular velocity discrepancy is positive, consistent with our hypothesis about the lift and the slip angular velocity discrepancy.

In figure XI.20, we consider the case of heavier than fluid particles $\rho_p / \rho_f = 1.005$ migrating at $R = 20$. For this relatively lightweight particle the equilibrium solutions are unique at $R = 20$ and the angular slip velocity discrepancy changes with the lift as the particle approaches $y_p = y_e$ from above or below.

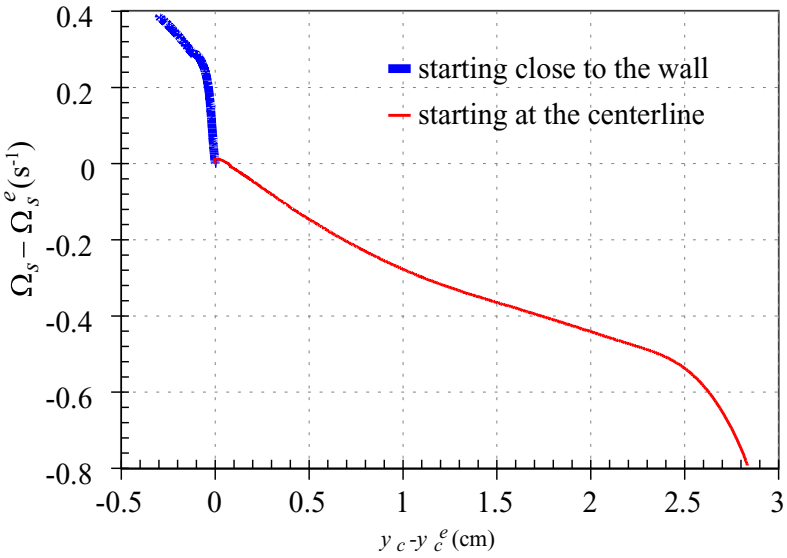

Figure XI.19. *Analysis on the angular slip velocity discrepancy in the case of multiple equilibrium ($\rho_p / \rho_f = 1.01$, $R = 20$). Case* (a) *particle released close to the wall: ($y_p(t=0) = 1.0$ cm). Case* (b) *particle released at the centerline: ($y_p(t=0) = 6.0$ cm). For this data, the buoyant weight intersects the lift force at three points, and two of them yield stable solutions (figure XI.8, table XI.1). For case* (a)*, the particle travels from a position close to the wall to the equilibrium height closer to the wall $y_e = 1.323$ cm, whereas for case* (b)*, the particle travels from the centerline to the equilibrium height far from the wall $y_e = 3.165$ cm. The discrepancy changes sign at the equilibrium $y_p = y_e$ where the lift balances the buoyant weight.*

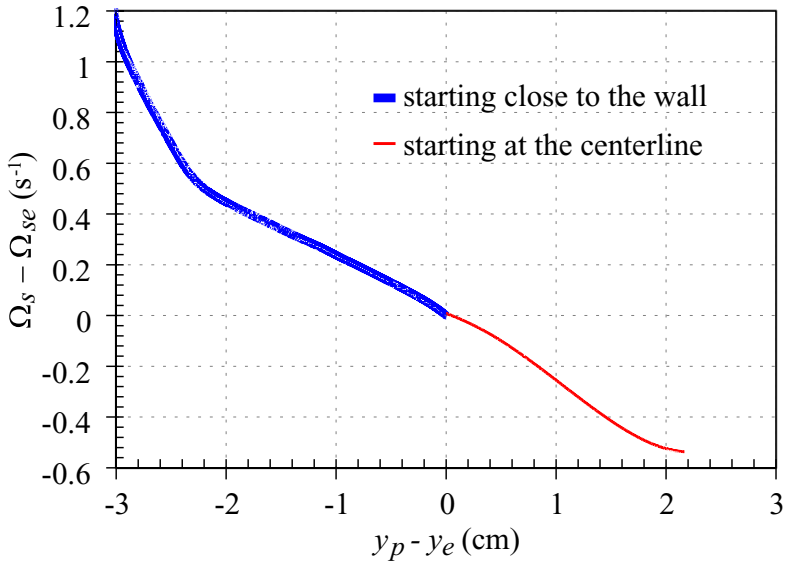

Figure XI.20*. Analysis on the angular slip velocity discrepancy in the case of unique equilibrium* ($\rho_p/\rho_f = 1.005$, $R = 20$)*. Case* (a)*, particle released close to the wall:* ($y_p(t=0) = 1.0$ *cm). Case* (b) *particle released at the centerline:* ($y_p(t=0) = 6.0$ *cm). For this data the buoyant weight intersects the lift force at only one point (figure XI.8, table XI.1). Therefore, no matter where the particle started it will reach the same equilibrium height at* $y_e = 3.834$ *cm. The discrepancy is positive if the local value is greater than the equilibrium value, and it is negative for the opposite condition. The angular slip velocity discrepancy changes its sign as the particle height discrepancy does.* Note*: the initial condition for all the cases was the following: First, to get a fully developed velocity profile, a simulation at the initial height* ($y_p(t=0) = 1.0$ *cm or* $y_p(t=0) = 6.0$ *cm) was performed using a constrained motion on the vertical direction. Secondly, the vertical motion constrain is released, and therefore the particle travels to a preferential equilibrium height.*

▪ Summary

The lift and migration of neutrally buoyant and heavier-than-liquid circular particles in a plane Poiseuille flow was studied using direct numerical simulation. The study looks at the relation of slip velocity and angular slip velocity to lift and migration. No matter where the neutrally bouyant particle is released, it will migrate to a unique equilibrium height and move forward with a unique steady particle velocity and rotate with unique steady angular velocity. Neutrally buoyant particles migrate to a radius which can be called the "Segré Silberberg" radius. This radius is a reference; heavier-than-liquid particles also migrate to an equilibrium radius that is close to the Segré-Silberberg radius if the particle density is close to the fluid density. The particles migrate to an equilibrium position y_e with shear rate $\dot{\gamma}_e$ such that the local fluid rotation $-\frac{1}{2}\dot{\gamma}_e$ is slightly greater than the particle angular velocity Ω_p. The angular slip velocity, $\Omega_s = \Omega_p + \frac{1}{2}\dot{\gamma}_e$ is always positive but at equilibrium it is very small; $\Omega_p \approx -\frac{1}{2}\dot{\gamma}_e$ can be proposed as an approximation. The slip velocity at equilibrium $U_s = U_{fe} - U_p$ is always positive and slowly varying.

Since the shear rate and slip velocities are one signed they do not explain why the lift changes sign across the equilibrium radius. We found that the quantity, which does change sign

at y_e, is the angular slip velocity discrepancy; the angular slip velocity minus the equilibrium angular slip velocity $\Omega_s - \Omega_{se}$. $\Omega_s - \Omega_{se} > 0$ when $y_p < y_e$ and $\Omega_s - \Omega_{se} < 0$ when $y_p > y_e$. The adjustment of the angular velocity of a free particle is very critical to lift. One might think of the angular velocity discrepancy as a shear flow analogue to the circulation in aerodynamic lift.

We derived a shear version of our long particle model. The long particle model arises when the circular particle is replaced with a long rectangle of the same diameter as the circle, but so long that we may neglect end effects. In the shear version we allow the rectangle to shear at the rate $-\frac{1}{2}\dot{\gamma}$ of the local rotation. Using this model we can find explicit expressions for the fluid rotation in which the velocity on either side of the long particle is matched by the fluid velocity; then we satisfy the particles equation of motion in which the shear stress force balances the pressure drop force. This leads to explicit expression for the velocity of the particle (XI.16) and the slip velocity (XI.20) that is always positive. The shear version of the long particle model is in good agreement with the results of numerical computation of the motion of a free circular particle at points of stable equilibrium, both with respect to the particle velocity and the fluid velocity on the cross-section containing the center of the circular particle.

The results given in this paper are for two dimensions. It remains to be seen how such results carry over to three dimensions. We note that the celebrated lift formula (X.1) is a two-dimensional result.

XI Slip velocity and lift at finite Reynolds numbers.....118
- Equilibrium positions of neutrally buoyant and heavy particles..... 118
- Mechanism for lift 119
- Numerical simulation of migration and lift..... 120
- Long particle model..... 121
- Slip velocities, angular slip velocities and lift for neutrally buoyant circular particles 127
- Slip velocities, angular slip velocities and lift for non-neutrally buoyant circular particles..... 130
- Summary..... 134

(DISCARD THIS PAGE (only used to generate table of contents)